ACS APPLIED MATERIALS & INTERFACES

Research Article

www.acsami.org

Systematic Investigation of Surface Modification by Organosiloxane Self-Assembled on Indium–Tin Oxide for Improved Hole Injection in Organic Light-Emitting Diodes

Yan Zhao, Lian Duan,* Deqiang Zhang, Guifang Dong, Juan Qiao, Liduo Wang, and Yong Qiu

Key Lab of Organic Optoelectronics and Molecular Engineering of Ministry of Education, Department of Chemistry, Tsinghua University, Beijing 100084, China

ABSTRACT: Various works on modification of the indium–tin oxide (ITO) substrate have been carried out so as to enhance hole injection in organic light-emitting devices. Herein, a simple and efficient approach to tuning the work function of the ITO substrate is described by surface modification of ITO with an organosiloxane self-assembled monolayer. The influences of the electronegativity on modification of the ITO substrate are systematically investigated by attaching electron-withdrawing groups (Cl, Br, and I) and an electron-donating group (NH_2) to the organosiloxane materials. The preparation and modification of the ITO substrate has been studied using primarily atomic force microscopy and X-ray photoelectron spectroscopy and vacuum–ultraviolet spectroscopy, and remarkable changes have been observed after modification. The device based on a 3Cl–Si–ITO-modified anode exhibits the best efficiency among the devices, better than the control devices based on bare ITO, UV-treated ITO, and even Cl–ITO.

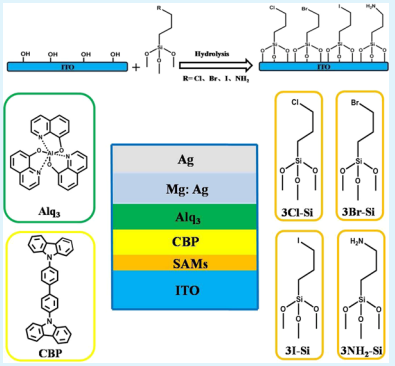

KEYWORDS: *organic light-emitting diodes, surface treatment, hole injection, self-assembled monolayer*

1. INTRODUCTION

Organic light-emitting diodes (OLEDs) have seen great development during the past 2 decades because of the advantages of self-emission, wide viewing angle, high efficiency, low driving voltage, and flexibility and potential applications in solid-state light sources, flat-panel displays, and even flexible displays.[1−3] Balanced electron and hole injection from the electrodes is crucial to high-efficiency OLEDs.[4] The large injection barrier between the work functions of the electrodes and the energy levels of organic materials would lead to poor charge injection, low efficiency, and fast degradation of OLEDs.[5] In particular, poor hole injection is caused by the large barrier of around 1 eV between the anode indium–tin oxide (ITO) with a work function of 4.7 eV and the commonly used hole-transport layer (HTL) and host materials.[6]

Remarkable works have been carried out on modification of the ITO substrate for the enhancement of hole injection. There are several methods that have been carried out to improve hole injection. (i) Plasma treatment or UV–ozone treatment. After pretreatment, the work function of ITO could be increased to over 6 eV, reducing the injection barrier to gain efficient hole injection.[7,8] (ii) Introduction of an interlayer between the ITO and HTL, such as hole injection layers (HILs) like poly(3,4-ethylenedioxythiophene):poly(styrenesulfonate) (PEDOT:PSS),[9] or metal oxide buffer layers like MoO_3.[10] (iii) Modification on the ITO surface, for example, tuning the surface work function of ITO with self-assembled monolayers (SAMs).[11−13] The SAMs formed on the ITO surface could tune the work function of ITO to improve the surface morphology of ITO and the adhesion characteristic at the ITO–organic functional film interface. An example is the work of Marks et al., in which ITO was modified with alkylsiloxane SAMs. Through a change in the length of the alkyl chain, the surface work function of ITO can be tuned, and the shorter the alkyl chain length, the better the device performance.[14] Recently, an effective method is reported by UV radiation of ITO with *o*-dichlorobenzene (*o*-DCB), which could obtain a monolayer of chlorinated ITO (Cl–ITO) and provide a direct match work function of >6.1 eV to the highest occupied molecular orbital (HOMO) of the commonly used hole-transport materials in the organic layer, without adding any functional layer. The improved efficiency is due to the high electronegativity of Cl on the ITO surface.[15] Later, Xu et al. also reported on an enhanced performance of polymer PV cells by dipping the ITO anode into a chloroform solution, due to the introduction of Cl species on the ITO surface.[16]

In this paper, we utilized the effect of high electronegative atoms on the ITO surface, combining the method of self-assembly of the organosiloxane materials on the ITO surface to modify the ITO anode. To fully understand the effect of electronegativity on the ITO surface, we introduced electron-withdrawing end groups (Cl, Br, and I) and an electron-donating group (NH_2) for the organosiloxane materials, obtaining a monolayer 3R–Si–ITO (R = Cl, Br, I, and NH_2) modified anode. Because of the high electronegativity of the end group Cl,

Received: January 19, 2014
Accepted: March 5, 2014
Published: March 5, 2014

   dx.doi.org/10.1021/am500399e | *ACS Appl. Mater. Interfaces* 2014, 6, 4570−4577

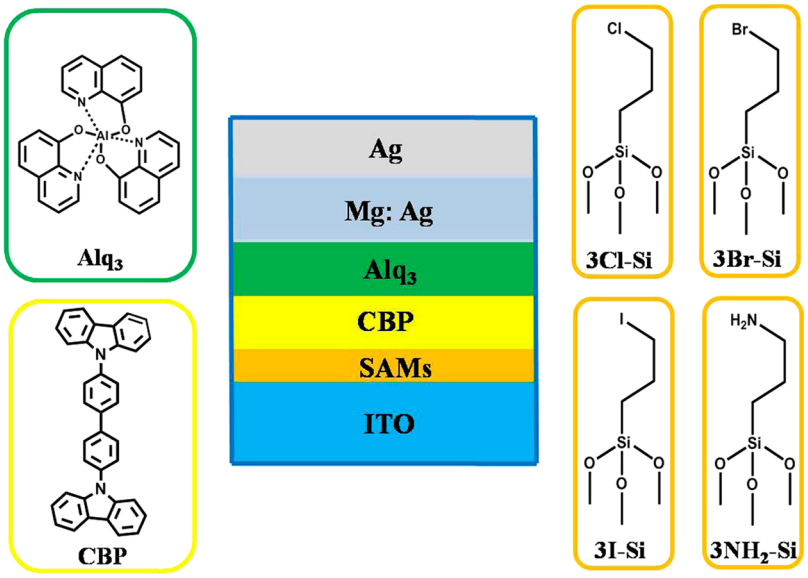

Figure 1. Device and chemical structures of materials used in the device fabrications.

Scheme 1. Scheme for ITO Surface Modification by Covalently Chemisorbed 3R−Si Materials

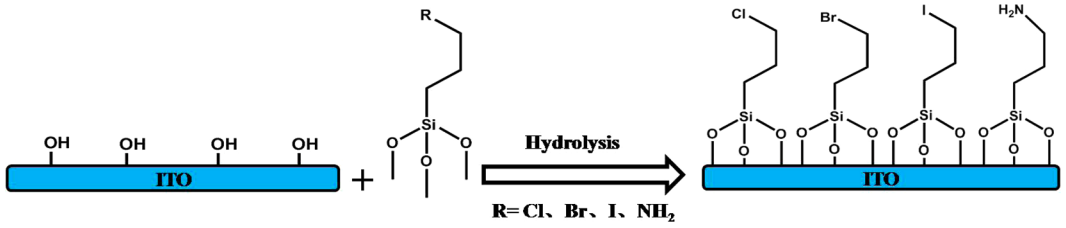

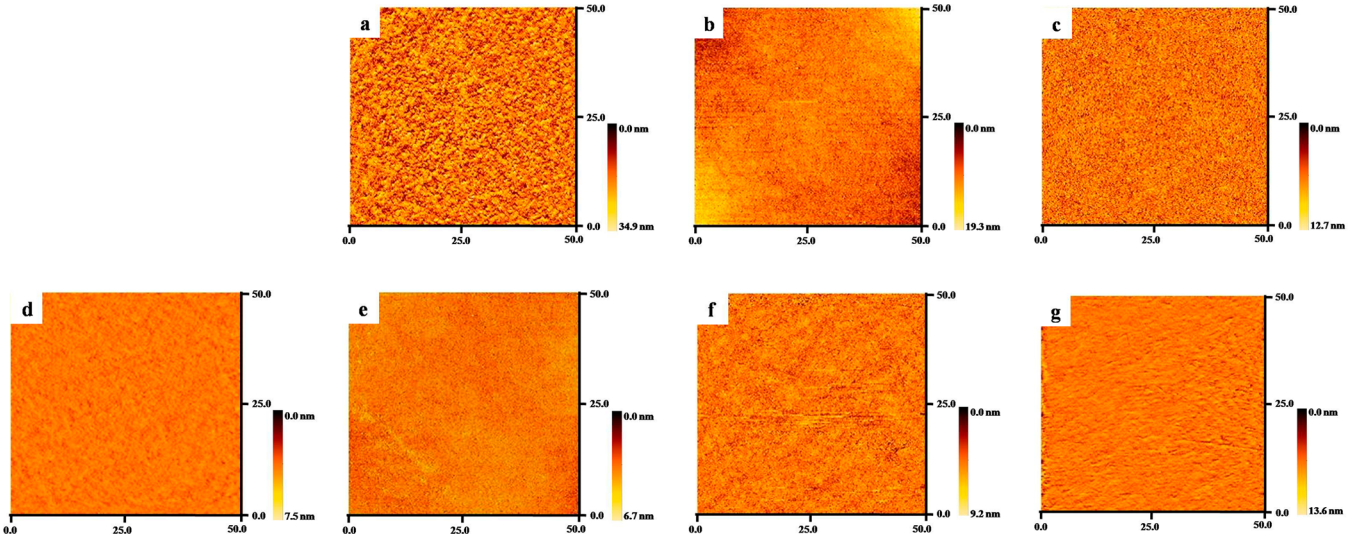

Figure 2. AFM images ($50 \times 50\ \mu m^2$) of the surface morphology of the pretreatment of ITO: (a) bare ITO; (b) UV−ITO; (c) Cl−ITO; (d) 3Cl−Si−ITO; (e) 3Br−Si−ITO; (f) 3I−Si−ITO; (g) $3NH_2$−Si−ITO.

the device with the 3Cl−Si−ITO anode exhibited the best performance among the devices.

2. MATERIALS AND METHODS

Self-Assembly of 3Cl−Si, 3Br−Si, 3I−Si, and $3NH_2$−Si on the ITO Substrate. The materials (3-chloropropyl)trimethoxysilane (3Cl−Si), (3-bromopropyl)trimethoxysilane (3Br−Si), (3-iopdopropyl)-trimethoxysilane (3I−Si), and (3-aminopropyl)trimethoxysilane ($3NH_2$−Si) for the self-assembly were purchased from the J K Chemical Company, as shown in Figure 1. For the self-assembly of 3R−Si on the ITO substrate (R = Cl, Br, I, and NH_2), the cleaned ITO substrates were immersed in a 1.0 mM dry toluene solution of 3Cl−Si, 3Br−Si, 3I−Si, and $3NH_2$−Si, respectively. Then, the substrates were rinsed with dry toluene and cleaned ultrasonically in isopropyl alcohol for 10 min, getting the SAMs on the ITO substrate, as shown in Scheme 1.

Surface Modification by UV Radiation Treatment on the ITO Substrate. In a general procedure, as for the common preparation of the ITO substrate, the ITO substrate was first cleaned in a series of lotions, then rinsed in deionized water three times, and baked by IR

dx.doi.org/10.1021/am500399e | ACS Appl. Mater. Interfaces 2014, 6, 4570−4577

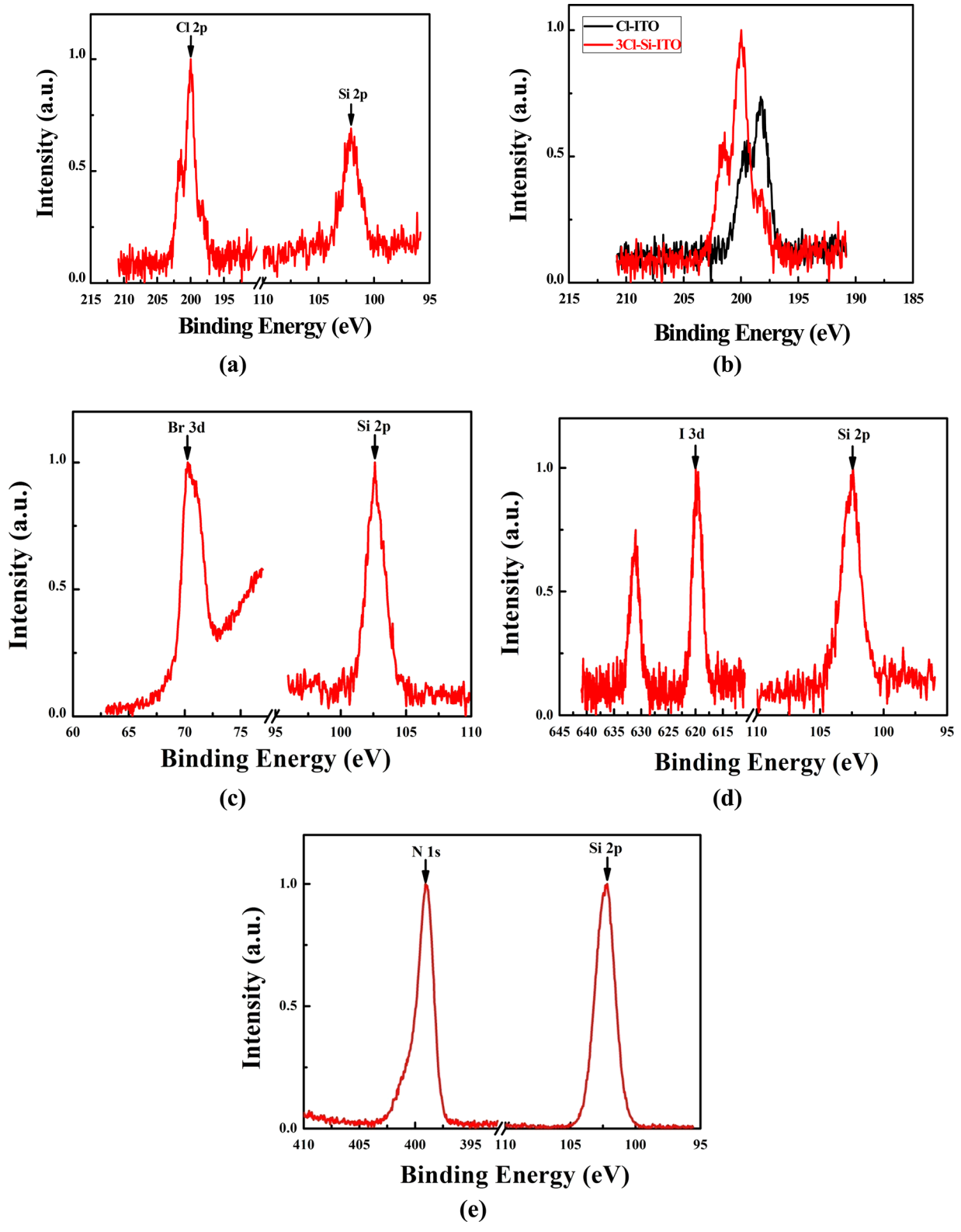

Figure 3. (a) XPS Cl 2p and Si 2p core-level spectra of 3Cl−Si−ITO. (b) XPS Cl 2p core-level spectra of 3Cl−Si−ITO and Cl−ITO, normalized to the Cl 2p peak of 3Cl−Si−ITO. (c) XPS Br 3d and Si 2p core-level spectra of 3Br−Si−ITO. (d) XPS I 3d and Si 2p core-level spectra of 3I−Si−ITO. (e) XPS N 1s and Si 2p core-level spectra of $3NH_2$−Si−ITO.

light. For the UV radiation treatment, the cleaned ITO substrate was exposured to UV−ozone for 10 min, obtaining the UV−ITO anode.

Surface Modification by UV Radiation Treatment with *o*-DCB on ITO Substrates. For Cl−ITO fabrication, the cleaned ITO substrate fully covered with *o*-DCB was treated by UV radiation for 10 min, and then the residual solvent was cleaned up, followed by exposure to UV−ozone for an additional 5 min to remove the rest fragments on the surface, obtaining the Cl−ITO anode.

Surface Morphology Characterization. The morphology of the self-assembly of 3R−Si on the ITO substrate was measured by scanning

dx.doi.org/10.1021/am500399e | *ACS Appl. Mater. Interfaces* 2014, 6, 4570−4577

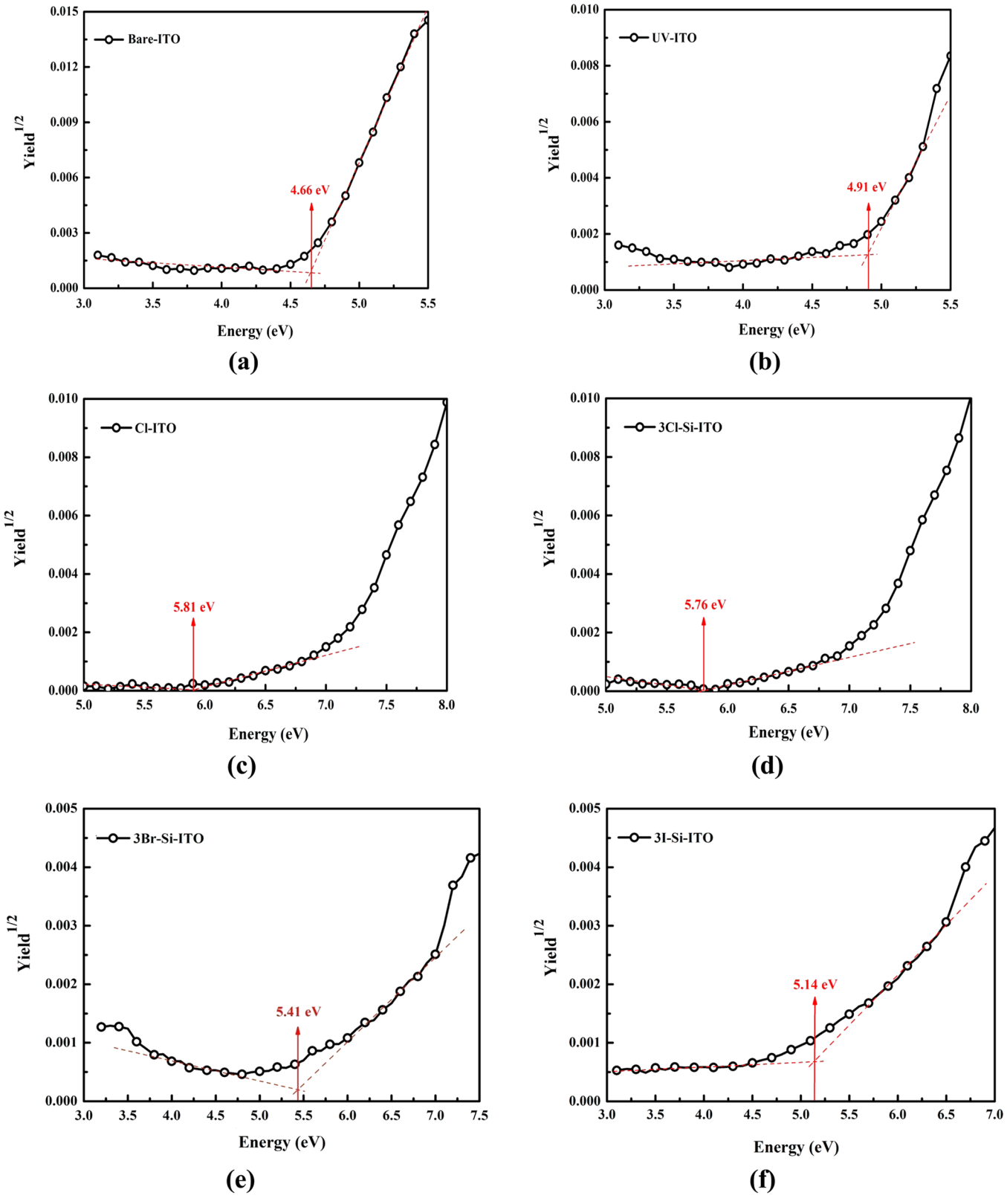

Figure 4. continued

dx.doi.org/10.1021/am500399e | *ACS Appl. Mater. Interfaces* 2014, 6, 4570−4577

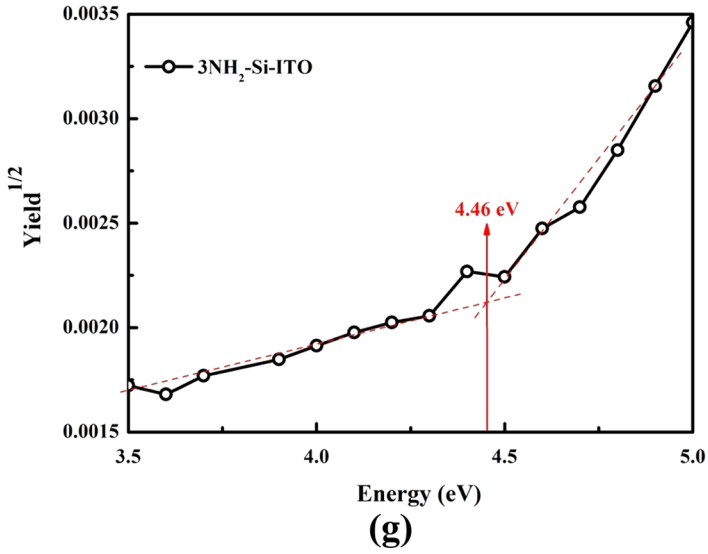

Figure 4. Vacuum−ultraviolet spectroscopy spectra of (a) bare ITO, (b) UV−ITO, (c) Cl−ITO, (d) 3Cl−Si−ITO, (e) 3Br−Si−ITO, (f) 3I−Si−ITO, and (g) $3NH_2$−Si−ITO.

electron microscopy and atomic force microscopy (AFM). Uniform films of the self-assembly of 3R−Si were observed over a 50 × 50 μm^2 scan area. As shown in Figure 2, the root-mean-square roughnesses (R_{rms}) are 2.47, 2.39, 2.73, and 2.93 nm, respectively, for 3Cl−Si, 3Br−Si, 3I−Si, and $3NH_2$−Si SAMs. For the bare ITO substrate, the R_{rms} is 4.64 nm. The surface morphologies of UV−ITO and Cl−ITO were also measured with R_{rms} values of 3.11 and 2.81 nm.

Chemical Characterization. The surface chemistry compositions of SAMs 3R−Si (R = Cl, Br, I, and NH_2) on ITO substrates were analyzed using the technology of X-ray photoelectron spectroscopy (XPS) and also for the sample of the Cl−ITO anode.

Measurement of the Ionization Potential for the Preprepared ITO Substrates. The ionization potentials of the preprepared ITO substrates were measured by vacuum−ultraviolet spectroscopy (PSY-202, Japan Sumitomo) in a vacuum chamber under a 1×10^{-2} Pa vacuum condition. The light sources were a xenon lamp of photon energy ranging from 3.0 to 5.0 eV and a deuterium lamp of photon energy ranging from 5.0 to 8.0 eV. For comparison, the ionization potentials of the 3R−ITO substrates were analyzed by the measurement. In addition, we also measured the ionization potentials of bare ITO, UV−ITO, and Cl−ITO for a thorough understanding.

Fabrication of OLEDs. We fabricated green-emission OLEDs with a structure of ITO/(4,40-*N*,*N*^{0}-dicarbazolebiphenyl) (CBP; 50 nm)/tris(8-hydroxyquinolinato)aluminum (Alq_3; 50 nm)/Mg:Ag (10:1, 150 nm)/Ag (50 nm) with different pretreatments for ITO substrates. After pretreatments, the ITO substrate was transferred to the vacuum evaporation chamber for evaporation of CBP, Alq_3, Mg, and Ag, respectively. The thicknesses of these materials were measured by AFM. The luminance−current characteristics of the devices were measured using a PR705 spectroscan spectrometer and the brightness (cd/m^2)−voltage (V), current density (A/m^2)−voltage (V), and efficiency (cd/A)−current density (A/m^2) characteristics were measured by a Keithley 4200 semiconductor characterization system.

3. RESULTS AND DISCUSSION

As shown in Figure 1, Alq_3-based OLEDs having the structure of ITO/CBP/Alq_3/Mg:Ag/Ag were fabricated, with Alq_3 as the electron-transport layer (ETL) and CBP as the HTL. The HOMO of CBP is deeper than the one of Alq_3, reported by Greiner et al., thus effectively reducing exciton quenching at the CBP/Alq_3 interface by accumulated radical holes.[17]

On the basis of modification of the self-assembly, 3R−Si−ITO (R = Cl, Br, I, and NH_2) substrates in the above OLEDs were investigated. The surface morphology of ITO plays a crucial role in the performance of OLEDs, and the smooth ITO substrate can guarantee formation of the perfect organic thin film to show excellent device performance. Therefore, we characterized the surface morphology of 3R−Si−ITO (R = Cl, Br, I, and NH_2) substrates by utilizing AFM. As shown in Figure 2, the R_{rms} values are 2.47, 2.39, 2.73, and 2.93 nm, respectively, for 3Cl−Si−ITO, 3Br−Si−ITO, 3I−Si−ITO, and $3NH_2$−Si−ITO. Upon comparison to a bare ITO surface with R_{rms} of 4.64 nm, we could learn that the surface morphology of ITO becomes smoother after modification. As to bare ITO, we mean that the surface of ITO is without any modification. For comparison, we also studied the OLEDs based on UV−ITO and Cl−ITO anodes, while the surface morphologies of UV−ITO and Cl−ITO were measured with R_{rms} of 3.11 and 2.81 nm.

After modification of the self-assembly, we investigated XPS studies on the 3Cl−Si−ITO substrate. The film was etched with ionic Ar, and the results are shown in Figure 3. The characteristic signatures of Cl 2p and Si 2p photoelectrons were observed from the 3Cl−Si−ITO anode, as shown in Figure 3a. For comparison, the surface for the Cl−ITO anode was also investigated by XPS technology. On the basis of the intensity of the Cl 2p peak for 3Cl−Si−ITO, the Cl 2p peak of the sample Cl−ITO was normalized. As shown in Figure 3b, we determine that the intensity of the Cl 2p peak of the 3Cl−Si−ITO sample is on the same order of magnitude as that of the sample of the Cl−ITO anode. This result explained that the surface formation of 3Cl−Si on the ITO anode is close to monolayer, the same as the sample of the Cl−ITO anode. The surface chemistry compositions of SAMs 3R−Si (R = Br, I, and NH_2) on the ITO substrates were also analyzed using the XPS technology, obtaining the characteristic peaks for the samples, as shown in Figure 3.

To fully understand the influences of the end group R for SAMs ITO, we investigated the ionization potentials of 3R−Si−ITO (R = Cl, Br, I, and NH_2) samples and also for bare ITO, UV−ITO, and Cl−ITO. As to the ionization potential, the energy that was required to remove an electron from an isolated atom or molecule is the definition of the ionization potential. In organic optoelectronics, the ionization potential is relative to the HOMO level of organic materials and the work function of ITO, determining the barrier for hole injection.[18] Figure 4 shows the curves of vacuum−ultraviolet spectroscopy of 3R−Si−ITO (R =

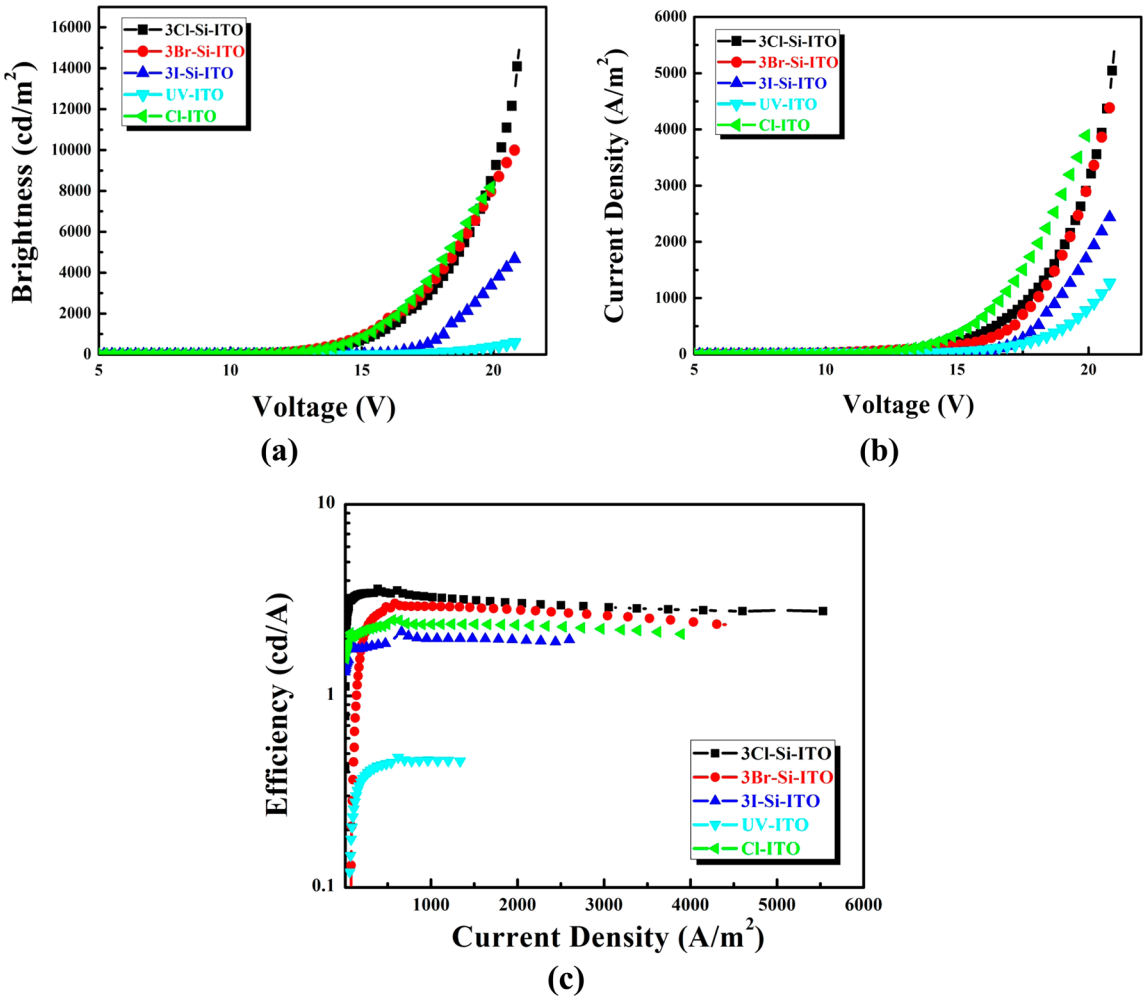

Figure 5. Curves of (a) brightness−voltage, (b) current density−voltage, and (c) efficiency−current density for OLEDs based on 3Cl−Si−ITO, 3Br−Si−ITO, 3I−Si−ITO, UV−ITO, and Cl−ITO anodes. Basic device structure: ITO/CBP (50 nm)/Alq_3 (50 nm)/Mg:Ag (150 nm)/Ag (50 nm).

Cl, Br, I, and NH_2), bare ITO, UV−ITO, and Cl−ITO. For 3R−Si−ITO (R = Cl, Br, I, and NH_2) samples, the ionization potentials are 5.76, 5.41, 5.14, and 4.46 eV respectively for 3Cl−Si−ITO, 3Br−Si−ITO, 3I−Si−ITO, and $3NH_2$−Si−ITO. As reported by Greiner et al., a deeper reason for the improved efficiency is the large difference in electronegativity between In and Cl (1.78 of In compared to 3.16 of Cl).[15] So the difference in electronegativity for the end group R is the main reason for the disparity of the ionization potentials. According to the inductive effects and electronegativity, the end groups could be classified into two types: electron-withdrawing and electron-donating groups. As for the halogen end groups R (Cl, Br, and I), these are generally regarded as the electron-withdrawing group that is beneficial to hole injection. By a comparison of the halogen end groups, the value of the electronegativity is Cl (3.16) > Br (2.96) > I (2.66),[19] which matches well with the ionization potentials of 3Cl−Si−ITO > 3Br−Si−ITO > 3I−Si−ITO samples. Also, the end group of NH_2 is defined as the electron-donating group and is bad at hole injection. Therefore, $3NH_2$−Si−ITO exhibited the lowest ionization potential among the above-mentioned samples. The ionization potential of bare ITO is 4.66 eV, and that for UV−ITO is 4.91 eV, as shown in Figure 4, with a large injection barrier still existing at the ITO/CBP interface, while the ionization potential is 5.81 eV for Cl−ITO, beneficial for hole injection at the ITO/CBP interface.

Herein, we fabricated a series of OLEDs with 3R−Si−ITO (R = Cl, Br, I, and NH_2) anodes to investigate the performances on the devices. To compare the performances of the devices with that of 3R−Si−ITO (R = Cl, Br, I, and NH_2) anodes, we also fabricated OLEDs with bare ITO, UV−ITO, and Cl−ITO anodes. Figure 5 shows the curves of the brightness (cd/m^2)−voltage (V), current density (A/m^2)−voltage (V), and efficiency (cd/A)−current density (A/m^2) for OLEDs based on 3R−Si−ITO (R = Cl, Br, I, and NH_2), bare ITO, UV−ITO, and Cl−ITO anodes. Because of the low work function of ITO, it is hard to realize hole injection from ITO to CBP without any modification, and the device based on the bare ITO anode showed no performance. As shown in Figure 5, OLEDs exhibited greater performance after modifications, especially for SAM ITO anodes. The maximum luminances are 15310 cd/m^2 (3Cl−Si−ITO), 10528 cd/m^2 (3Br−Si−ITO), and 5118 cd/m^2 (3I−Si−ITO). Also, the maximum efficiencies are 3.67, 3.14, and 2.16 cd/A for 3Cl−Si−ITO, 3Br−Si−ITO, and 3I−Si−ITO, respectively, while the device of the $3NH_2$−Si−ITO anode showed no device performance. It can be easily noticed that exhibitions of the devices based on SAM ITO anodes correspond well with the ionization potentials of 3R−Si−ITO (R = Cl, Br, I, and NH_2) samples. These results further indicated the influence of the end group R on modifications on 3R−Si−ITO (R = Cl, Br, I, and NH_2) anodes. We also obtain the performances of the devices

dx.doi.org/10.1021/am500399e | ACS Appl. Mater. Interfaces 2014, 6, 4570−4577

Table 1. Device Performances for OLEDs Based on 3R−Si−ITO (R = Cl, Br, I, and NH_2), bare ITO, UV−ITO, and Cl−ITO Anodes [Basic Device Structure: ITO/CBP (50 nm)/Alq_3 (50 nm)/Mg:Ag (150 nm)/Ag (50 nm)]

pretreatment	L^a [cd/m^2]	L^b [cd/m^2]	$\eta_L{}^a$ [cd/A]	$\eta_L{}^b$ [cd/A]	$\eta_p{}^a$ [lm/W]	$\eta_p{}^b$ [lm/W]	V_{on} (V)
bare ITO							
3Cl−Si−ITO	15310	3338	3.67	3.28	0.82	0.58	8.7
3Br−Si−ITO	10528	2990	3.14	2.94	0.62	0.53	8.8
3I−Si−ITO	5118	2014	2.16	1.99	0.37	0.33	9.6
3NH_2−Si−ITO							
UV−ITO	675	470	0.50	0.46	0.08	0.07	12.4
Cl−ITO	12447	2337	3.00	2.37	0.59	0.45	8.9

[a]Maximum values. [b]At 100 mA/cm^2.

based on UV−ITO and Cl−ITO anodes. The maximum luminances are 675 cd/m^2 (UV−ITO) and 12447 cd/m^2 (Cl−ITO). Also, the maximum efficiencies are 0.50 and 3.00 cd/A for UV−ITO and Cl−ITO, respectively. Compared to the device using the UV−ITO anode, the Cl−ITO-based device exhibited much better performance because of the effect of Cl atoms on the ITO surface. Compared to the device using the Cl−ITO anode, the 3Cl−Si−ITO-based device exhibited better performance. Although the ionization potential of Cl−ITO is a bit larger, the better performance for the 3Cl−Si−ITO-based device may be due to more charge balance. We also compared the current density (A/m^2)−voltage (V) curves for the devices, which gave insight into the hole injection efficiency at the ITO/CBP interface. As shown in Figure 5b, the current density of 3R−Si−ITO (R = Cl, Br, and I)-based devices exhibits a gradual change under the same voltage. The 3Cl−Si−ITO-based device shows the largest, and the 3I−Si−ITO-based device has the worst, indicating the influence of the end group R on the hole injection efficiency, while exhibition of the current density of the Cl-ITO-based device was larger than those of 3R−Si−ITO (R = Cl, Br, and I)-based devices and smaller than that of the UV-ITO-based device. The performances of those devices are listed in Table 1.

To deeply understand the influence of the end group NH_2 for hole injection, we compared the current (I)−voltage (V) curves of the Alq_3-based OLEDs with the different anodes of 3NH_2−Si−ITO and bare ITO, which helps to estimate the barrier height at the ITO/CBP interface. The larger the current the device exhibits under the same voltage, the lower the barrier height is. A lower barrier height is beneficial for hole injection. Because of the large injection barrier at the ITO/CBP interface, 3NH_2−Si−ITO- and bare-ITO-based devices exhibited no performance. As shown in Figure 6, the current of the 3NH_2−Si−ITO-based device is much lower than that of bare ITO, indicating that the hole injection barrier is increased by modification of the 3NH_2−Si SAMs on the ITO surface. This result further demonstrates the influence of the electronegativity on the work function of ITO: that in the system of SAMs, the introduction of the electron-withdrawing group with high electronegativity is beneficial for hole injection, while the effect of the electron-donating group is destructive to hole injection. Also, the ionization potential of 3NH_2−Si−ITO obtained is 4.46 eV, shown in Figure 4, even lower than the ionization potential of bare ITO. This distinction deeply elucidated the reason for the terrible performance of the 3NH_2−Si−ITO-based device. Although the low ionization potential of 3NH_2−Si is not suitable for the anode, it has potential applications for the electrode in inverted organic optoelectronic devices.[20−22]

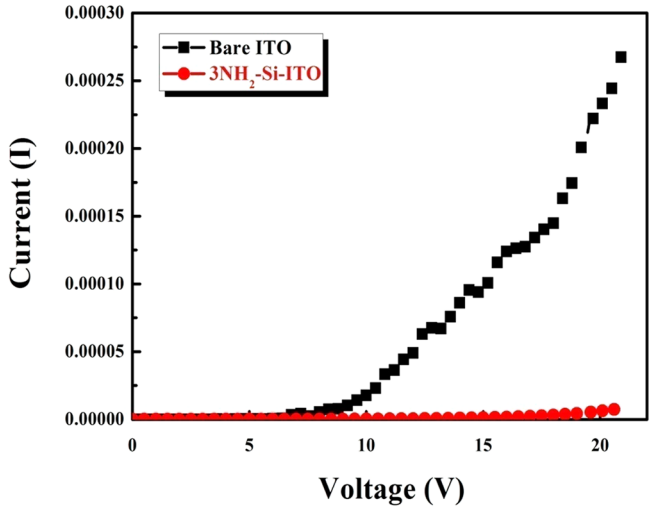

Figure 6. Comparison of the current−voltage for OLEDs based on 3NH_2−Si−ITO and bare ITO anodes. Basic device structure: ITO/CBP (50 nm)/Alq_3 (50 nm)/Mg:Ag (150 nm)/Ag (50 nm).

4. CONCLUSION

In summary, we have demonstrated a simple and efficient approach to the self-assembly of 3R−Si materials (R = Cl, Br, I, and NH_2) to modify the ITO anode by utilizing the effect of atoms with high electronegativity. Using the technology of AFM and XPS and measurement of the ionization potential, we have presented here a systematic investigation of the influence of the electronegativity on the work function of ITO, by introducing electron-withdrawing and electron-donating groups. Meanwhile, a series of devices based on 3R−Si−ITO anodes showed various performances because of the influence of the electronegativity for the end groups. Moreover, the device based on the 3Cl−Si−ITO anode exhibited better efficiency compared to the devices based on the Cl−ITO and UV−ITO anodes. We believe the approach we demonstrate here would be useful for the application of OLEDs in display and lighting.

AUTHOR INFORMATION

Corresponding Author

*E-mail: duanl@mail.tsinghua.edu.cn. Tel: (008610) 62779988. Fax: (008610) 62795137.

Notes

The authors declare no competing financial interest.

■ ACKNOWLEDGMENTS

This research was supported by the National Natural Science Foundation of China (Grants 51173096, 61177023, and 21161160447).

■ REFERENCES

(1) Kido, J.; Kimura, M.; Nagai, K. Multilayer White Light-Emitting Organic Electroluminescent Devices. *Science* **1995**, *267*, 1332−1334.
(2) D'Andrade, B. W.; Forrest, S. R. White Organic Light-Emitting Devices for Solid-State Lighting. *Adv. Mater.* **2004**, *16*, 1585−1595.
(3) Sun, Y.; Giebink, N. C.; Kanno, H.; Ma, B.; Thompson, M. E.; Forrest, S. R. Management of Singlet and Triplet Excitons for Efficient White Organic Light-emitting Devices. *Nature* **2006**, *440*, 908−12.
(4) Ma, H.; Yip, H.-L.; Huang, F.; Jen, A. K. Y. Interface Engineering for Organic Electronics. *Adv. Funct. Mater.* **2010**, *20*, 1371−1388.
(5) Qiao, X.; Tao, Y.; Wang, Q.; Ma, D.; Yang, C.; Wang, L.; Qin, J.; Wang, F. Controlling Charge Balance and Exciton Recombination by Bipolar Host in Single-layer Organic Light-emitting Diodes. *J. Appl. Phys.* **2010**, *108*, 034508.
(6) Zhao, Y.; Duan, L.; Zhang, D.; Qiao, J.; Wang, L.; Qiu, Y. Performance Enhancement of Organic Light-emitting Diodes by Chlorinated Indium Tin Oxide in the Presence of Hydrogen Peroxide. *Org. Electron.* **2013**, *14*, 882−887.
(7) Kim, J. S.; Granström, M.; Friend, R. H.; Johansson, N.; Salaneck, W. R.; Daik, R.; Feast, W. J.; Cacialli, F. Indium−tin Oxide Treatments for Single- and Double-layer Polymeric Light-emitting Diodes: The Relation between the Anode Physical, Chemical, and Morphological Properties and the Device Performance. *J. Appl. Phys.* **1998**, *84*, 6859.
(8) So, S. K.; Choi, W. K.; Cheng, C. H.; Leung, L. M.; Kwong, C. F. Surface Preparation and Characterization of Indium Tin Oxide Substrates for Organic Electroluminescent Devices. *Appl. Phys. A: Mater. Sci. Process.* **1999**, *68*, 447−450.
(9) Elschner, A.; Bruder, F.; Heuer, H. W.; Jonas, F.; Karbach, A.; Kirchmeyer, S.; Thurm, S. PEDT/PSS for Efficient Hole-injection in Hybrid Organic Light-emitting Diodes. *Synth. Met.* **2000**, *111*, 139−143.
(10) Shrotriya, V.; Li, G.; Yao, Y.; Chu, C.-W.; Yang, Y. Transition Metal Oxides as the Buffer Layer for Polymer Photovoltaic Cells. *Appl. Phys. Lett.* **2006**, *88*, 073508.
(11) Huang, Q. L.; Evmenenko, G.; Dutta, P.; Marks, T. J. Molecularly "Engineered" Anode Adsorbates for Probing OLED Interfacial Structure−Charge Injection/Luminance Relationships: Large, Structure-Dependent Effects. *J. Am. Chem. Soc.* **2003**, *125*, 14704−14705.
(12) Malinsky, J. E.; Jabbour, G. E.; Shaheen, S. E.; Anderson, J. D.; Richter, A. G.; Marks, T. J.; Armstrong, N. R.; Kippelen, B.; Dutta, P.; Peyghambarian, N. Self-Assembly Processes for Organic LED Electrode Passivation and Charge Injection Balance. *Adv. Mater.* **1999**, *11*, 227−231.
(13) Huang, Q. L.; Li, J. F.; Evmenenko, G. A.; Dutta, P.; Marks, T. J. Systematic Investigation of Nanoscale Adsorbate Effects at Organic Light-Emitting Diode Interfaces. Interfacial Structure−Charge Injection−Luminance Relationships. *Chem. Mater.* **2006**, *18*, 2431−2442.
(14) Huang, Q. L.; Evmenenko, G. A.; Dutta, P.; Lee, P.; Armstrong, N. R.; Marks, T. J. Covalently Bound Hole-Injecting Nanostructures. Systematics of Molecular Architecture, Thickness, Saturation, and Electron-Blocking Characteristics on Organic Light-Emitting Diode Luminance, Turn-on Voltage, and Quantum Efficiency. *J. Am. Chem. Soc.* **2005**, *127*, 10227−10242.
(15) Helander, M. G.; Wang, Z. B.; Qiu, J.; Greiner, M. T.; Puzzo, D. P.; Liu, Z. W.; Lu, Z. H. Chlorinated Indium Tin Oxide Electrodes with High Work Function for Organic Device Compatibility. *Science* **2011**, *332*, 944−947.
(16) Xu, Z. Q.; Li, J.; Yang, J. P.; Cheng, P. P.; Zhao, J.; Lee, S. T.; Li, Y. Q.; Tang, J. X. Enhanced Performance in Polymer Photovoltaic Cells with Chloroform Treated Indium Tin Oxide Anode Modification. *Appl. Phys. Lett.* **2011**, *98*, 253303.
(17) Wang, Z. B.; Helander, M. G.; Qiu, J.; Liu, Z. W.; Greiner, M. T.; Lu, Z. H. Direct Hole Injection in to 4,4′-*N*,*N*′-dicarbazole-biphenyl: A Simple Pathway to Achieve Efficient Organic Light Emitting Diodes. *J. Appl. Phys.* **2010**, *108*, 024510.
(18) Liu, X.; Dong, G.; Duan, L.; Wang, L.; Qiu, Y. High Performance Low-voltage Organic Phototransistors: Interface Modification and the Tuning of Electrical, Photosensitive and Memory Properties. *J. Mater. Chem.* **2012**, *22*, 11836.
(19) Murphy, L. R.; Meek, T. L.; Allred, A. L.; Allen, L. C. Evaluation and Test of Pauling's Electronegativity Scale. *J. Phys. Chem. A* **2000**, *104*, 5867−5871.
(20) Zhou, Y.; Fuentes-Hernandez, C.; Shim, J.; Meyer, J.; Giordano, A. J.; Li, H.; Winget, P.; Papadopoulos, T.; Cheun, H.; Kim, J.; Fenoll, M.; Dindar, A.; Haske, W.; Najafabadi, E.; Khan, T. M.; Sojoudi, H.; Barlow, S.; Graham, S.; Bredas, J. L.; Marder, S. R.; Kahn, A.; Kippelen, B. A Universal Method to Produce Low-Work Function Electrodes for Organic Electronics. *Science* **2012**, *336*, 327−32.
(21) Xiong, T.; Wang, F. X.; Qiao, X. F.; Ma, D. G. A Soluble Nonionic Surfactant as Electron Injection Material for High-efficiency Inverted Bottom-emission Organic Light Emitting Diodes. *Appl. Phys. Lett.* **2008**, *93*, 123310.
(22) Chen, J. S.; Shi, C. S.; Fu, Q.; Zhao, F. C.; Hu, Y.; Feng, Y. L.; Ma, D. G. Solution-processable Small Molecules as Efficient Universal Bipolar Host for Blue, Green and Red Phosphorescent Inverted OLEDs. *J. Mater. Chem.* **2012**, *22*, 5164.